ISSN 1330-3651 (Print), ISSN 1848-6339 (Online)
https://doi.org/10.17559/TV-20231226001235
Original scientific paper

Modelling of Flank and Crater Wear during Dry Turning of AISI 316L Stainless Steel as a Function of Tool Geometry Using the Response Surface Design

Djordje VUKELIC*, Katica SIMUNOVIC, Vitalii IVANOV, Mario SOKAC, Vladimir KOCOVIC, Zeljko SANTOSI, Goran SIMUNOVIC

Abstract: The article investigates the influence of geometric parameters of CVD cutting inserts on flank and crater wear during dry turning. Turning of AISI 316L stainless steel was performed with different values of approach angles, rake angles, clearance angles, inclination angles and corner radii. After dry turning, the flank and crater wear of the cutting inserts were measured. The effects of the input parameters on the output parameters were evaluated using ANOVA. The results of the experiments showed that the flank and crater wear increases with increasing approach angle, rake angle, clearance angle, inclination angle and decreasing corner radius. Based on the test results, statistical models were developed to predict the distribution of flank and crater wear using the response surface design. The absolute and percentage errors obtained show that the models developed can be successfully used to predict flank and crater wear.

Keywords: crater wear; dry turning; flank wear

1 INTRODUCTION

Turning is a process for pre-machining or finishing mostly cylindrical workpieces. Turning is used to machining workpieces made of various materials such as wood, plastic, cast iron, steel, etc [1, 2]. One of the most commonly used materials for the manufacture of fittings, pumps, heat exchangers, condensers, evaporators, tanks, cisterns, pipes, etc. is 316L stainless steel. This steel is characterized by a higher creep resistance, excellent formability and weldability, fracture and tensile strength at high temperatures as well as corrosion and pitting resistance. The turning of workpieces made of AISI 316L stainless steel has been the subject of numerous theoretical, simulative and experimental studies.

Valiorgue et al. [3] predicted residual stresses during turning of 316L stainless steel. This method models the thermo-mechanical load on the machined surface. Leppert [4] presented research results on the machining process and described the topographical surface properties obtained during dry turning and turning with minimum quantity lubrication (MQL) turning of AISI 316L steel. The test results showed a significant influence of the cutting zone environment and the cutting parameters on the cutting force, surface roughness, profile bearing ratio and the occurrence of surface defects. Saketi et al. [5] studied the influence of tool surface topography on the initiation and build-up of transfer layers during turning of 316L stainless steel. The results show that the transfer tendency of work material is strongly influenced by the surface topography of the rake face. The build-up of transfer layers is localised on the rake face. It was also found that an improved surface finish reduces the coating wear and consequently the crater wear rate of the inserts investigated. Basmacia and Ay [6] used the grey relational analysis optimization method to evaluate the influences of feed rate, depth of cut and cooling system on surface roughness, cutting force and material hardness after turning AISI 316L stainless steel with conventional and wiper inserts. Nur et al. [7] investigated the effects of cutting speed and feed on cutting force, surface roughness, power consumption and tool life. Cutting speed was proportional to power consumption and inversely proportional to tool life and showed no significant effect on cutting force and surface roughness. Feed was proportional to cutting force, power consumption and surface roughness and inversely proportional to tool life. Sathishkumar and Rajmohan [8] carried out optimization of machining parameters during turning to minimize surface roughness and cutting temperature. Feed had a greater impact on the response variables, followed by depth of cut, type of cutting fluid and spindle speed. Struzikiewicz et al. [9] presented the analysis of the influence of turning data on cutting force, surface roughness and maximum temperature values in the cutting zone during turning of 316L steel produced by 3D printing. Saketi et al. [10] studied the wear of three different cemented carbide grades during turning of AISI 316L. It was found that the wear rates depend not only on the cutting speed but also on the grain size. The degradation of cemented carbide at higher cutting speeds is mainly controlled by diffusion wear. Zaharudin and Budin [11] investigated the influence of cutting speed on coated cutting tools when dry turning of AISI 316L stainless steel. The surface roughness of the workpiece decreases, while the wear rate of the cutting tool increases with the increase in cutting speed. Elkaseer et al. [12] investigated chip formation and surface generation during turning of 316L stainless steel. A finite element method (FEM) was used to simulate the turning process of stainless steel. The results of the FEM were used to determine the optimal cutting parameters that enable a suitable cutting mechanism, higher quality of the machined surface and higher productivity. Singh and Sinha [13] investigated tool wear, cutting forces and surface roughness during dry machining of AISI 316L with coated carbide tools and four input variables such as cutting speed, feed, depth of cut and corner radius. Touggui et al. [14] determined the influence of cutting parameters such as cutting speed, feed and depth of cut on surface roughness (Ra) and material removal rate (MRR) during dry turning of AISI 316L with cermet insert. The most important parameter influencing Ra was feed, while MRR was strongly influenced by depth of cut, followed by cutting speed and feed. Barari et al. [15] investigated the magnitude and morphology of tool wear under four types of lubrication (MQL, MQCL, dry and wet) when turning 316L steel. The composition of the

material adhering to the cutting tools showed that a built-up edge occurred with all lubrication types. MQCL resulted in a longer tool life compared to the other three lubrication types. Touggui et al. [16] optimized the surface roughness and cutting force for a range of values for cutting speed, feed and depth of cut in dry turning of AISI 316L using two different cutting inserts, namely cermet and coated carbide inserts. Dumas et al. [17] investigated the machining-induced surface integrity when turning a fillet radius in a 316L stainless steel. The average uncut chip thickness is the most important parameter for surface integrity. Del Risco-Alfonso et al. [18] studied the dependence between the main cutting force, the initial wear rate of the cutting tool, the surface roughness and the cutting parameters when turning AISI 316L. A multi-objective optimization model was proposed to minimize the consumed energy and initial wear rate of the cutting tool and maximize productivity. Benmeddour [19] presented a numerical study on the impact of tool geometry such as rake angle and cutting edge radius on the temperature distribution and residual stresses in the machining surface of AISI 316L stainless steel. Martowibowo and Damanik [20] presented the application of genetic algorithm optimization for MRR and Ra of AISI 316L in dry turning. Cutting speed, feed and depth of cut had a significant influence on MRR, while feed and depth of cut had a large effect on Ra. Leksyckiet al. [21] presented the results of an investigation of the plastic side flow of 316L stainless steel in the finish turning under dry cutting conditions. The effect of cutting speed and feed on the intensity of side flow was analysed. Szczotkarz et al. [22] investigated the advantages of applying the MQL and MQCL methods to reduce the wear of the AlTiN-coated cutting tool. In the MQL method, the active medium is a vegetable oil that increases the lubricating properties of the cutting fluid, while in the MQCL method, the active medium is a mixture of water and a mineral oil-based emulsion concentrate that increases the cooling properties of the cutting fluid. Benkhelifa et al. [23] presented the effects of various parameters such as cutting speed, feed and depth of cut on surface roughness and tool flank wear when turning of AISI 316L. The surface roughness was largely influenced by the feed, while the cutting speed had the greatest influence on tool flank wear. Maruda et al. [24] focused on the importance of selecting the appropriate concentration and size of copper nanoparticles to be introduced into the MQL machining method, taking into account the effects of machining vibrations and surface topography. Natesh et al. [25] dealed with the tribological and morphological study on optimization and microscopic analysis of machined surface in turning of AISI 316 stainless steel under MQL application with five different lubricants (oil–water emulsion, mineral oil, simarouba oil, pongam oil and neem oil). Bjerke et al. [26] studied the interaction of the coating with adhering steel and inclusions in a (Ti,Al)N coated tool. The study examines the differences across the rake face of the tool. Moreno et al. [27] investigated the failure wear mechanisms of cathodically deposited coatings on cutting inserts during low-speed turning of 316L stainless steel. The predominant coating wear mechanism is adhesive wear due to fracture. Oussama et al. [28] studied the effects of nanoparticle type, lubrication method, cutting speed and feed on surface roughness, feed force and cutting temperature in MQL turning of AISI 316L.

As can be seen, various methods have been developed for analysing the turning process of 316L stainless steel. The effects of turning parameters (cutting speed, feed and depth of cut), cooling lubricant, coatings and similar factors on the turning results, such as surface topography, surface layer properties, material removal rate, tool wear morphology, chip formation, etc., were investigated. The investigations were carried out under both dry and wet conditions, but a considerable number of investigations were devoted to the study of the turning process under minimum quantity lubrication and minimum quantity cooling lubrication conditions.

The main disadvantage of dry turning is the lower quality of the machined surface and the shorter tool life. However, compared to alternative turning methods, the process is cleaner and certain costs are lower (cost of buying the fluid, cost of treating the fluid, cost of disposing of the fluid, etc.). Dry turning can lead to higher wear of the cutting tools due to the high cutting temperatures, which can have a negative impact on the quality of the machined surface and results in higher costs, the need for reworking, etc. It is therefore very important to determine the input parameters with which the required operation can be carried out, both from the point of view of machining and from the point of view of the negative impact on the environment. Dry machining can be achieved by selecting suitable machine tools, fixtures and cutting tools, while taking into account the characteristics of the workpiece. It is necessary to use machine tools with high performance and accuracy, rigid fixtures that ensure reliable locating and secure clamping, and it is preferable to use cutting tools with a coating and suitable geometry so that the tribological effects are more favourable. During dry machining, high friction occurs at the contact point of the cutting tool on one side with the chips and the workpiece on the other side, i.e. high temperatures and high contact pressures occur. Such machining conditions create specific phenomena in the cutting zone that can lead to an increase in cutting tool wear, which in turn can have negative effects on accuracy, quality, costs, etc. Therefore, under dry turning conditions, special attention must be paid to the choice of cutting tool geometry.

In contrast to the previous studies, the aim of this study is to evaluate the influence of five input parameters of the turning process that are related to the geometry of the cutting tool. The input parameters to be considered are: approach angle (κ), rake angle (γ), clearance angle (α), inclination angle (λ) and corner radius (r). The output parameters to be considered are the flank wear (VB) and crater wear (KB) of the cutting insert.

2 METHODOLOGY

The methodology according to which the study was conducted is shown in Fig. 1.

The tests were conducted on AISI 316L stainless steel with the following chemical composition: 17% chromium (Cr), 12% nickel (Ni), 2.50% molybdenum (Mo), 2.00% manganese (Mn), 0.90% silicon (Si), 0.10% nitrogen (N), 0.03% carbon (C), 0.02% sulphur (S), 0.045% phosphorus (P), balance iron (Fe). The most important properties of

this stainless steel are modulus of elasticity 200 GPa, tensile strength 485 MPa, Brinell hardness 217, density 8.0 kg/m^3, thermal conductivity 15 W/m K.

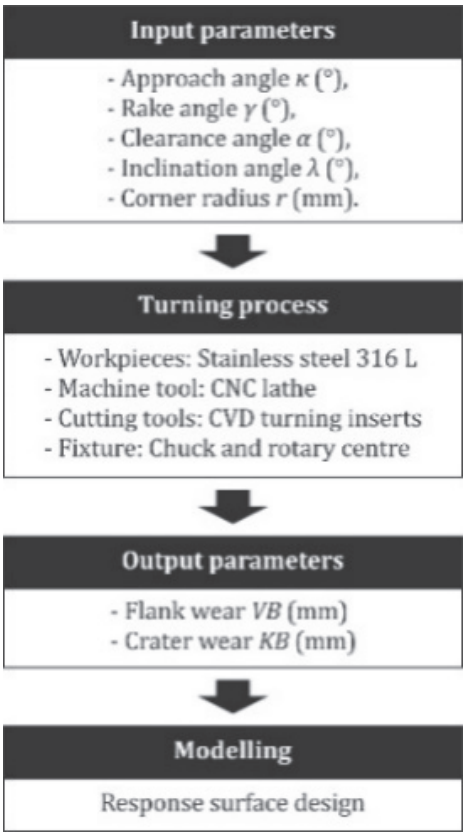

Figure 1 Research methodology

The turning operation on workpieces with dimensions of Ø40 × 400 mm was carried out on the Mori Seiki CNC lathe, which is characterized by excellent rigidity and high accuracy and precision. Locating and clamping of workpieces was performed using a chuck and rotary centre.

Based on the workpiece material, the type of machining (external longitudinal turning) and the machining conditions (stable machining), the following common features were selected in accordance with the recommendations: insert shape code S, insert thickness 4.8 mm, cutting edge effective length 12.3 mm, inscribed circle diameter 12.7 mm, substrate HC, coating CVD TiCN + Al_2O_3 + TiN.

In accordance with the recommendations of the insert manufacturer, experimental tests were conducted with the following machining parameters: depth of cut a_p = 0.4 mm, feed f = 0.1 mm/rev and cutting speed v_c = 210 m/min.

Five input parameters were varied during the study, the values of which are listed in Tab. 1.

After the experimental investigation, flank wear (*VB*) and crater wear (*KB*) were measured. The wear measurements were carried out using an Alicona non-contact 3D optical microscope (Fig. 2).

Table 1 Input parameter levels

Parameter	Level 1	Level 2	Level 3
Approach angle κ / °	45	-	90
Rake angle γ / °	3	6	9
Clearance angle α / °	3	5	7
Inclination angle λ / °	−3	0	3
Corner radius r / mm	0.2	0.4	0.8

Figure 2 Wear measurement

After the measurements, the turning process was modelled using response surface design. When the response surface design was built, the discrete type of factors was used.

In addition to the statistical analyses, the modelling performance was evaluated by calculating the percentage error (*PE*), absolute error (*AE*), mean percentage error (*MPE*) and mean absolute error (*MAE*):

$$PE_x = \frac{\left|x_{ipv} - x_{imv}\right|}{x_{imv}} \cdot 100\% \qquad x = VB, KB \qquad (1)$$

$$AE_x = \left|x_{ipv} - x_{imv}\right| \qquad x = VB, KB \qquad (2)$$

$$MPE_x = \frac{1}{n}\sum_{i=1}^{n} \frac{\left|x_{ipv} - x_{imv}\right|}{x_{imv}} \cdot 100\% \quad x = VB, KB \qquad (3)$$

$$MAE_x = \frac{1}{n}\sum_{i=1}^{n} \left|x_{ipv} - x_{imv}\right| \qquad x = VB, KB \qquad (4)$$

where: x_{ipv} - predicted value for the i-th experiment, x_{imv} - measured value for the i-th experiment, and n is the total number of experiments.

3 RESULTS

The experimental studies were conducted in the form of a full factorial experiment. A total of 162 experiments were carried out. The measurement results for various combinations of input parameters are listed in Tab. 2.

Now follows the statistical processing and analysis of the experimental data, first for the flank wear (*VB*) and then for the crater wear (*KB*).

After processing the experimental data (Design Expert, version 22.0.6) for the flank wear (*VB*), the proposed linear regression model was selected on the basis of various statistical indicators (model significance p-value, lack of fit p-value, R^2, adjusted R^2, predicted R^2). Tab. 3 presents the analysis of variance (ANOVA) for the selected linear model, which shows that the model is significant and that all factors are significant (p-values are less than 0.1).

Table 2 Results of the measurement

Run Order	κ / °	γ / °	α / °	λ / °	r / mm	VB / mm	KB / mm	Run Order	κ / °	γ / °	α / °	λ / °	r / mm	VB / mm	KB / mm
1	90	9	7	0	0.8	0.338	1.034	82	45	9	5	3	0.4	0.282	0.994
2	90	9	7	0	0.2	0.358	1.116	83	45	9	3	3	0.8	0.257	0.935
3	90	6	3	0	0.2	0.244	0.991	84	90	6	5	−3	0.8	0.233	0.908
4	90	3	7	−3	0.8	0.279	0.889	85	45	9	5	3	0.8	0.269	0.958
5	45	3	5	3	0.2	0.233	0.919	86	90	3	5	−3	0.8	0.226	0.855
6	90	3	7	−3	0.4	0.292	0.925	87	45	3	3	−3	0.8	0.196	0.747
7	90	6	5	3	0.4	0.251	1.011	88	45	3	3	0	0.8	0.199	0.771
8	90	9	5	−3	0.8	0.282	0.976	89	45	6	3	3	0.2	0.228	0.949
9	45	9	5	3	0.2	0.289	1.040	90	45	6	3	−3	0.4	0.216	0.836
10	90	3	3	−3	0.4	0.227	0.868	91	90	3	3	−3	0.2	0.234	0.914
11	45	9	3	3	0.4	0.270	0.971	92	90	6	5	0	0.2	0.256	1.014
12	45	9	3	0	0.2	0.275	0.974	93	90	9	7	3	0.4	0.353	1.113
13	90	6	7	3	0.2	0.311	1.091	94	90	6	7	0	0.8	0.289	0.966
14	90	6	5	3	0.2	0.258	1.057	95	45	9	7	3	0.8	0.322	0.992
15	45	9	7	−3	0.8	0.317	0.925	96	90	3	5	−3	0.2	0.246	0.937
16	90	3	7	0	0.2	0.302	0.995	97	90	9	7	−3	0.2	0.355	1.092
17	45	9	3	3	0.2	0.277	1.017	98	45	3	7	−3	0.8	0.261	0.804
18	90	9	3	−3	0.2	0.290	1.035	99	90	6	7	0	0.2	0.309	1.048
19	45	3	5	−3	0.4	0.221	0.806	100	45	6	3	0	0.8	0.206	0.824
20	90	6	3	3	0.4	0.239	0.988	101	90	6	3	0	0.4	0.237	0.945
21	45	9	3	−3	0.4	0.265	0.904	102	90	9	7	3	0.2	0.360	1.159
22	45	9	3	0	0.8	0.255	0.892	103	45	6	7	3	0.4	0.286	0.960
23	45	9	5	0	0.2	0.287	0.997	104	90	9	3	3	0.8	0.275	1.020
24	45	6	5	−3	0.4	0.228	0.859	105	45	9	7	−3	0.2	0.337	1.007
25	45	6	7	3	0.8	0.273	0.924	106	90	9	7	0	0.4	0.351	1.070
26	90	9	3	3	0.4	0.288	1.056	107	90	6	3	−3	0.2	0.241	0.967
27	90	9	3	−3	0.4	0.283	0.989	108	90	9	7	−3	0.8	0.335	1.010
28	90	6	5	0	0.4	0.249	0.968	109	90	9	7	3	0.8	0.340	1.077
29	90	3	7	0	0.4	0.295	0.949	110	90	3	3	3	0.8	0.219	0.899
30	45	3	3	−3	0.2	0.216	0.829	111	45	9	7	0	0.4	0.333	0.985
31	90	6	7	3	0.8	0.291	1.009	112	45	6	7	0	0.2	0.291	0.963
32	45	3	7	3	0.8	0.266	0.871	113	45	6	5	3	0.4	0.233	0.926
33	45	3	3	0	0.2	0.219	0.853	114	45	6	7	−3	0.4	0.281	0.893
34	45	6	5	−3	0.8	0.215	0.823	115	45	3	3	3	0.2	0.221	0.896
35	90	3	7	−3	0.2	0.299	0.971	116	45	3	5	−3	0.8	0.208	0.770
36	90	9	5	0	0.8	0.285	1.002	117	45	6	3	3	0.8	0.208	0.867
37	45	3	3	−3	0.4	0.209	0.783	118	45	3	5	0	0.4	0.224	0.830
38	45	3	5	3	0.4	0.226	0.873	119	45	6	3	3	0.4	0.221	0.903
39	90	3	3	3	0.4	0.232	0.935	120	45	3	5	3	0.8	0.213	0.837
40	45	9	5	−3	0.8	0.264	0.891	121	90	3	7	3	0.4	0.297	0.992
41	90	6	7	0	0.4	0.302	1.002	122	90	9	3	0	0.8	0.273	0.977
42	45	3	3	0	0.4	0.212	0.807	123	45	3	5	0	0.8	0.211	0.794
43	90	6	5	−3	0.2	0.253	0.990	124	45	6	3	−3	0.8	0.203	0.800
44	45	9	3	0	0.4	0.268	0.928	125	90	3	5	3	0.2	0.251	1.004
45	90	6	7	3	0.4	0.304	1.045	126	90	3	3	3	0.2	0.239	0.981
46	90	3	5	0	0.8	0.229	0.879	127	90	6	7	−3	0.2	0.306	1.024
47	45	6	7	0	0.4	0.284	0.917	128	45	3	3	3	0.8	0.201	0.814
48	90	9	3	−3	0.8	0.270	0.953	129	45	6	5	0	0.8	0.218	0.847
49	90	6	5	0	0.8	0.236	0.932	130	90	3	5	0	0.2	0.249	0.961
50	45	3	7	0	0.8	0.264	0.828	131	90	9	3	3	0.2	0.295	1.102
51	45	9	3	−3	0.2	0.272	0.950	132	90	6	3	3	0.8	0.226	0.952
52	45	6	7	−3	0.8	0.268	0.857	133	90	3	5	0	0.4	0.242	0.915
53	45	6	7	0	0.8	0.271	0.881	134	90	6	5	3	0.8	0.238	0.975
54	45	6	7	3	0.2	0.293	1.006	135	90	6	3	−3	0.4	0.234	0.921
55	45	6	3	−3	0.2	0.223	0.882	136	90	6	3	0	0.8	0.224	0.909
56	90	3	7	3	0.2	0.304	1.038	137	45	3	7	3	0.4	0.279	0.907
57	45	9	5	−3	0.4	0.277	0.927	138	90	3	5	−3	0.4	0.239	0.891
58	90	9	5	0	0.2	0.305	1.082	139	90	3	3	−3	0.8	0.214	0.832
59	45	6	5	3	0.8	0.220	0.890	140	90	6	7	−3	0.4	0.299	0.978
60	45	3	7	0	0.4	0.277	0.864	141	90	6	7	−3	0.8	0.286	0.942
61	45	9	7	3	0.2	0.342	1.074	142	90	9	3	0	0.2	0.293	1.059
62	90	9	5	−3	0.4	0.295	1.012	143	45	6	5	−3	0.2	0.235	0.905
63	45	6	7	−3	0.2	0.288	0.939	144	45	9	7	0	0.2	0.340	1.031
64	45	3	7	−3	0.2	0.281	0.886	145	45	9	5	0	0.4	0.280	0.951
65	45	3	5	0	0.2	0.231	0.876	146	45	3	7	−3	0.4	0.274	0.840
66	45	6	5	0	0.2	0.238	0.929	147	45	9	5	0	0.8	0.267	0.915
67	90	6	5	−3	0.4	0.246	0.944	148	90	3	3	0	0.8	0.217	0.856
68	90	6	3	3	0.2	0.246	1.034	149	45	6	5	3	0.2	0.240	0.972
69	90	3	3	0	0.2	0.237	0.938	150	90	9	5	3	0.2	0.307	1.125
70	45	9	7	0	0.8	0.320	0.949	151	45	9	3	−3	0.8	0.252	0.868
71	90	3	3	0	0.4	0.230	0.892	152	90	9	5	−3	0.2	0.302	1.058
72	45	6	5	0	0.4	0.231	0.883	153	45	6	3	0	0.4	0.219	0.860

Table 2 Results of the measurement (continuation)

Run Order	κ / °	γ / °	α / °	λ / °	r / mm	VB / mm	KB / mm	Run Order	κ / °	γ / °	α / °	λ / °	r / mm	VB / mm	KB / mm
73	45	3	3	3	0.4	0.214	0.850	154	90	9	3	0	0.4	0.286	1.013
74	90	9	5	3	0.4	0.300	1.079	155	45	3	7	0	0.2	0.284	0.910
75	90	9	7	−3	0.4	0.348	1.046	156	90	9	5	3	0.8	0.287	1.043
76	45	9	7	3	0.4	0.335	1.028	157	90	6	3	−3	0.8	0.221	0.885
77	90	3	5	3	0.8	0.231	0.922	158	45	3	7	3	0.2	0.286	0.953
78	45	6	3	0	0.2	0.226	0.906	159	90	3	7	0	0.8	0.282	0.913
79	90	3	5	3	0.4	0.244	0.958	160	45	9	5	−3	0.2	0.284	0.973
80	45	9	7	−3	0.4	0.330	0.961	161	45	3	5	−3	0.2	0.228	0.852
81	90	9	5	0	0.4	0.298	1.036	162	90	3	7	3	0.8	0.284	0.956

Table 3 ANOVA for linear model - flank wear (*VB*)

Source	Sum of Squares	df	Mean Square	F-value	p-value	
Model	0.2237	5	0.0447	224.98	< 0.0001	significant
A - Corner radius	0.0111	1	0.0111	55.93	< 0.0001	
B - Inclination angle	0.0007	1	0.0007	3.39	0.0673	
C - Clearance angle	0.1141	1	0.1141	573.72	< 0.0001	
D - Rake angle	0.0847	1	0.0847	425.85	< 0.0001	
E - Approach angle	0.0131	1	0.0131	66	< 0.0001	
Residual	0.031	156	0.0002			
Cor Total	0.2547	161				

The statistical indicators of the model are shown in Tab. 4. The predicted R^2 of 0.8695 agrees well with the adjusted R^2 of 0.8743, i.e. the difference is less than 0.2. The Adeq precision measures the signal-to-noise ratio. A ratio of more than 4 is desirable. The ratio of 60.408 indicates a reasonable signal. From the previous analysis, it can be concluded that the proposed model is suitable for good predictions about the flank wear (*VB*).

Table 4 Statistical indicators of the model - flank wear (*VB*)

R^2	0.8782
Adjusted R^2	0.8743
Predicted R^2	0.8695
Adeq Precision	60.4078

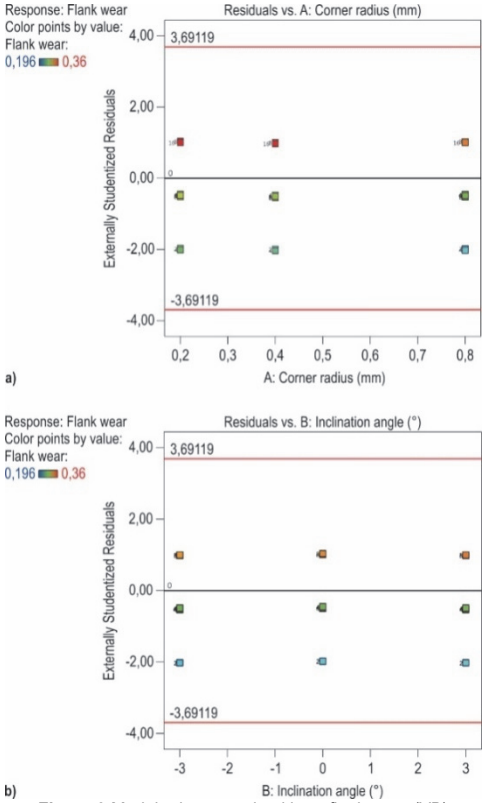

Figure 3 Model adequacy checking - flank wear (VB)
a) Externally studentized residuals vs. corner radius levels; b) Externally studentized residuals vs. inclination angle levels

And the analysis of the externally studentized residuals showed that the model is adequate. There are minor deviations (patterns) in the dependence of the residuals on the clearance and rake angle. Fig. 3 shows a graphical representation of externally studentized residuals vs. corner radius levels (a) and externally studentized residuals vs. inclination angle levels (b).

Using the linear regression model (Eq. (5)) and Fig. 4, it can be seen that flank wear decreases with increasing corner radius and increases with increasing tool angles (see Figs. 4a and 4b).

$$VB = 0.116583 - 0.033214 \cdot r + 0.000833 \cdot \lambda + 0.01625 \cdot \alpha + 0.009333 \cdot \gamma + 0.0004 \cdot \kappa \quad (5)$$

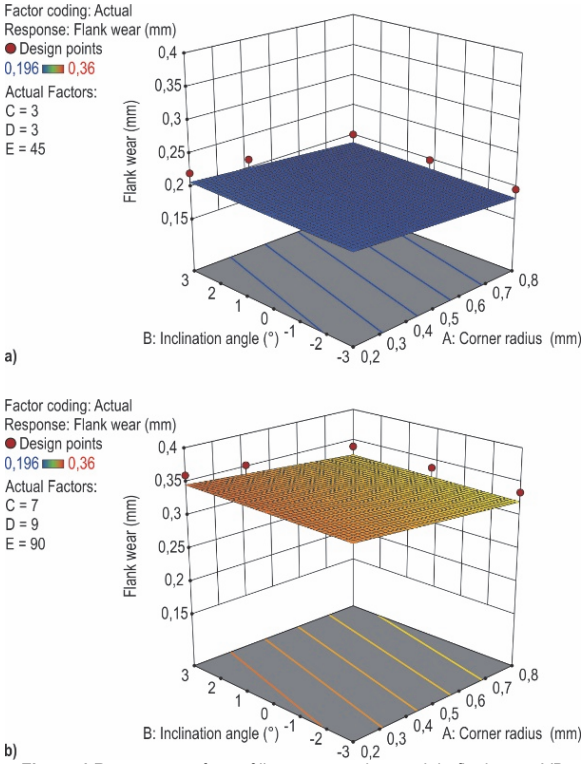

Figure 4 Response surface of linear regression model - flank wear VB
a) The lowest levels of factors C, D and E, b) The highest levels of factors C, D and E

The following is the analysis of variance (ANOVA) for the proposed linear regression model for crater wear (*KB*), Tab. 5, which shows that the model is significant, as are all factors.

Table 5 ANOVA for linear model - crater wear (*KB*)

Source	Sum of Squares	df	Mean Square	F-value	p-value	
Model	1.07	5	0.2135	1805.21	< 0.0001	significant
A - Corner radius	0.1702	1	0.1702	1439	< 0.0001	
B - Inclination angle	0.1212	1	0.1212	1024.87	< 0.0001	
C - Clearance angle	0.0877	1	0.0877	741.77	< 0.0001	
D - Rake angle	0.3955	1	0.3955	3344.68	< 0.0001	
E - Approach angle	0.2928	1	0.2928	2475.71	< 0.0001	
Residual	0.0184	156	0.0001			
Cor Total	1.09	161				

Similar to flank wear (*VB*), statistical indicators are also given for this model (Tab. 6) and some of the graphical presentations of the model adequacy checking (Fig. 5). Finally, the regression Eq. (6) in relation to the actual factors and a graphical representation (contours), Fig. 6, are given.

Table 6 Statistical indicators of the model - crater wear (KB)

R^2	0.983
Adjusted R^2	0.9825
Predicted R^2	0.9818
Adeq Precision	194.9588

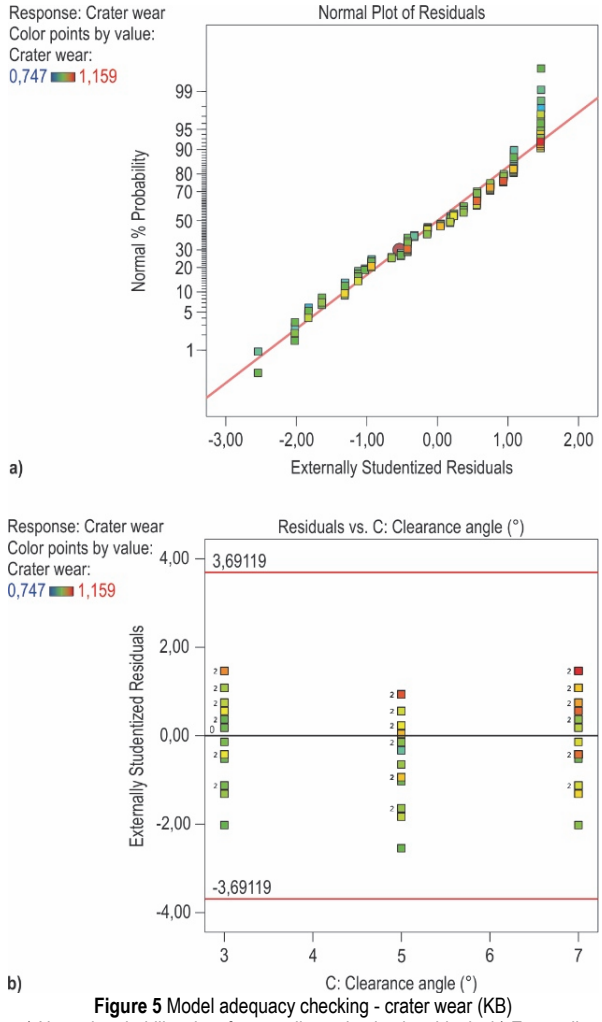

Figure 5 Model adequacy checking - crater wear (KB)
a) Normal probability plot of externally studentized residuals; b) Externally studentized residuals vs. clearance angle levels

$$KB = 0.684657 - 0.129934 \cdot r + 0.011167 \cdot \lambda + 0.01425 \cdot \alpha + 0.020173 \cdot \gamma + 0.001889 \cdot \kappa \quad (6)$$

As with flank wear (*VB*), it can be seen from Eq. (2) and Fig. 6 that crater wear (*KB*) decreases as the corner radius increases and that crater wear (*KB*) increases as the angles of the cutting inserts increase.

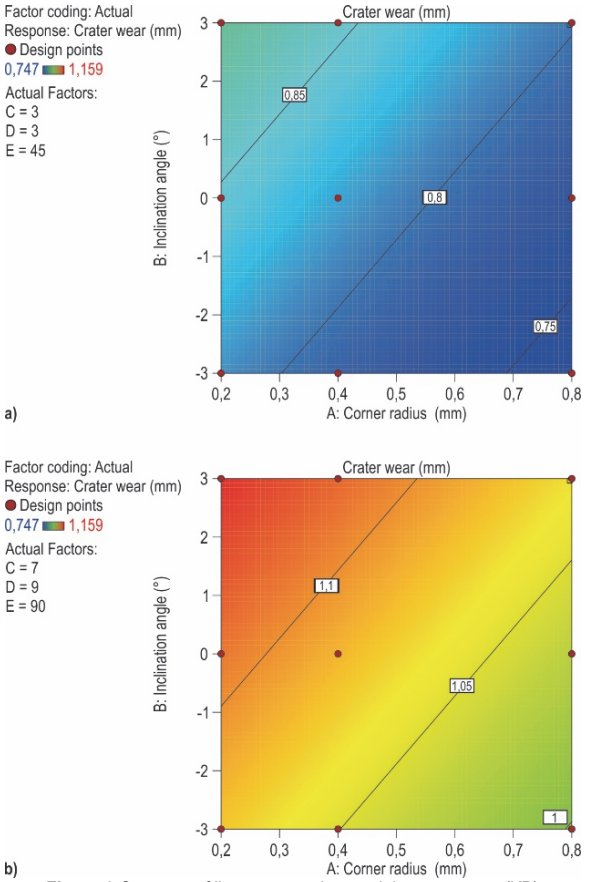

Figure 6 Contours of linear regression model - crater wear (KB)
a) The lowest levels of factors C, D and E; b) The highest levels of factors C, D and E

Table 7 Coefficients of linear correlation between response and factors

Parameter	Flank wear	Crater wear
Approach angle	0.227	0.519
Rake angle	0.577	0.604
Clearance angle	0.669	0.284
Inclination angle	0.051	0.334
Corner radius	−0.209	−0.396

A comparison of the linear correlation coefficients for both responses can be found in Tab. 7. It can be seen that the correlation for all angles of the cutting inserts is positive for both responses, with the correlation between flank wear and inclination angle being the lowest. In addition, the correlation with the corner radius is negative for both responses. The analysed statistical indicators

confirm the above conclusions. The similar influence of all five factors on both responses can also be confirmed by the linear correlation coefficient between responses, which is 0.77.

4 DISCUSSION

The descriptive parameters of experimental results are listed in Tab. 8. The results indicate a significant dispersion considering that the values for flank wear range from 0.119 mm to 0.341 mm and with a ratio between the maximum and minimum values of 1.84, and the values for crater wear range from 0.747 mm to 1.159 mm and with a ratio between the maximum and minimum values of 1.55. This shows that the geometric parameters of the cutting insert can significantly influence wear and that their appropriate combination can increase the tool life of the cutting tools. From the results obtained, it can be concluded that the flank and crater wear decreases with a decrease in the approach angle, the rake angle, the clearance angle and the inclination angle as well as with an increase in the corner radius.

Table 8 Descriptive parameters of experimental results

Parameter	Flank wear / mm	Crater wear / mm
Minimum value	0.196	0.747
Mean value	0.265	0.944
Maximum value	0.360	1.159
Standard deviation	0.040	0.082
Ratio	1.84	1.55

With an increase in the approach angle, the length of the chip contact increases with a simultaneous decrease in the chip thickness. The cutting forces are distributed over a greater length of the cutting edge, so that the wear on the insert is less. The rake angle has a major influence on chip disposal, cutting temperature and tool life, especially in dry machining. As the rake angle increases, the strength of the cutting edge decreases. Therefore, wear also increases as the rake angle increases. The clearance angle prevents friction between the clearance surface and the workpiece. The greater the clearance angle, the less likely contact between the clearance surface and the workpiece is. However, as the clearance angle increases the strength of the cutting edge decreases and wear increases. The inclination angle has an effect on the direction of chip removal and less on the wear of the cutting tool. Negative values of the inclination angle increase the strength of the cutting edge, therefore wear is lower. The corner radius has a major influence on the surface roughness. As the corner radius increases, the strength of the cutting edge also increases, so that wear on the flank and rake face decreases. With a larger corner radius, the length of the contact between the cutting tool and the workpiece increases. As a result, the heat is distributed over a larger surface area and the concentrated tool wear is reduced, which contributes to lower flank and crater wear.

As seen from Tab. 9, the percentage prediction errors range from 2.033 to 7.136% for flank wear (*VB*) and from 0.000 to 3.058% for crater wear (*KB*). These percentage errors correspond to absolute errors in the range of 0.006 - 0.028 mm for flank wear (*VB*) and in the range of 0.000 - 0.027 mm for crater wear (*KB*).

Table 9 Prediction errors

Parameter	Flank wear		Crater wear	
	Absolute error / mm	Percentage error / %	Absolute error / mm	Percentage error / %
Minimum	0.006	2.033	0.000	0.000
Mean	0.012	3.905	0.009	0.939
Maximum	0.028	7.136	0.027	3.058

The values of the determined errors are within acceptable limits and show the possibility of practical implementation of the regression equations in a real production environment.

5 CONCLUSION

In the study, the parameters of the geometry of the cutting inserts were modelled from the point of view of tool life, i.e. flank and crater wear. The results obtained show that dry turning of 316L stainless steel can be performed with smaller values of approach angle, rake angle, clearance angle and inclination angle and with larger values of corner radius from the point of view of increasing tool life.

The limitation of the study is that the results obtained can be applied to the range of input parameters under which the experiments were carried out. In order to achieve greater universality of the developed model, experimental investigations are planned on workpieces with different mechanical, physical and thermal properties as well as on tools with different geometric and technological characteristics. Future research will also focus on modelling a larger number of variables, i.e. including a larger number of input parameters and output parameters of the process in the model. Finally, future research is planned to investigate wear mechanisms, chip morphology, etc.

Acknowledgements

This research was funded by the University of Slavonski Brod, Republic of Croatia (project SmartPRO) and by the Ministry of Science, Technological Development and Innovation, Republic of Serbia (project number 451-03-47/2023-01/200156).

6 REFERENCES

[1] Tomov, M., Gecevska, V., & Vasileska, E. (2022). Modelling of multiple surface roughness parameters during hard turning: A comparative study between the kinematical-geometrical copying approach and the design of experiments method (DOE). *Advances in Production Engineering & Management*, *17*(1), 75-88. https://doi.org/10.14743/apem2022.1.422

[2] Vukelic, D., Simunovic, K., Kanovic, Z., Saric, T., Doroslovacki, K., Prica, M., & Simunovic, G. (2022). Modelling surface roughness in finish turning as a function of cutting tool geometry using the response surface method, Gaussian process regression and decision tree regression. *Advances in Production Engineering & Management*, *17*(3), 367-380. https://doi.org/10.14743/apem2022.2.433

[3] Valiorgue, F., Rech, J., Hamdi, H., Gilles, P., & Bergheau, J. M. (2007). A new approach for the modelling of residual stresses induced by turning of 316L. *Journal of Materials Processing Technology*, *191*(1-3), 270-273. https://doi.org/10.1016/j.jmatprotec.2007.03.021

[4] Leppert, T. (2012). Surface layer properties of AISI 316L steel when turning under dry and with minimum quantity lubrication conditions. *Proceedings of the Institution of Mechanical Engineers, Part B: Journal of Engineering Manufacture*, *226*(4), 617-631. https://doi.org/10.1177/0954405411429894

[5] Saketi, S., Östby, J., & Olsson, M. (2016). Influence of tool surface topography on the material transfer tendency and tool wear in the turning of 316L stainless steel. *Wear*, *368-369*, 239-252. https://doi.org/10.1016/j.wear.2016.09.023

[6] Basmacia, G. & Ay, M. (2017). Optimization of cutting parameters, condition and geometry in turning AISI 316L stainless steel using the Grey-based Taguchi method. *Acta Physica Polonica A*, *131*(3), 354-358. https://doi.org/10.12693/APhysPolA.131.354

[7] Nur, R., Noordin, M. Y., Izman, S., & Kurniawan, D. (2017). Machining parameters effect in dry turning of AISI 316L stainless steel using coated carbide tools. *Proceedings of the Institution of Mechanical Engineers, Part E: Journal of Process Mechanical Engineering*, *231*(4), 676-683. https://doi.org/10.1177/0954408915624861

[8] Sathishkumar, S. D. & Rajmohan, T. (2018). Multi-Response Optimization of Machining Parameters in CNC Turning of AISI 316L Stainless Steel Using MQL Nano fluids. *IOP Conference Series: Materials Science and Engineering*, *390*(1), art. no. 012049. https://doi.org/10.1088/1757-899X/390/1/012049

[9] Struzikiewicz, G., Zębala, W., Matras, A., Machno, M., Ślusarczyk, Ł., Hichert, S., & Laufer, F. (2019). Turning research of additive laser molten stainless steel 316L obtained by 3D printing. *Materials*, *12*(1), art. no. 182. https://doi.org/10.3390/ma12010182

[10] Saketi, S., Bexell, U., Östby, J., & Olsson, M. (2019). On the diffusion wear of cemented carbides in the turning of AISI 316L stainless steel. *Wear*, *430-431*, 202-213. https://doi.org/10.1016/j.wear.2019.05.010

[11] Zaharudin, A.M. & Budin, S. (2019). Influence of cutting speed on coated TiCN cutting tool during turning of AISI 316L stainless steel in dry turning process. *IOP Conference Series: Materials Science and Engineering*, *505*(1), art. no. 012044. https://doi.org/10.1088/1757-899X/505/1/012044

[12] Elkaseer, A., Abdelaziz, A., Saber, M., & Nassef, A. (2019). FEM-based study of precision hard turning of stainless steel 316L. *Materials*, *12*(16), art. no. 2522. https://doi.org/10.3390/ma12162522

[13] Singh, A. & Sinha, M. K. (2020). Multi-Response Optimization during Dry Turning of Bio-implant Steel (AISI 316L) Using Coated Carbide Inserts. *Arabian Journal for Science and Engineering*, *45*(11), 9397-9411. https://doi.org/10.1007/s13369-020-04717-x

[14] Touggui, Y., Belhadi, S., Mechraoui, S.-E., Uysal, A., Yallese, M. A., & Temmar, M. (2020). Multi-objective optimization of turning parameters for targeting surface roughness and maximizing material removal rate in dry turning of AISI 316L with PVD-coated cermet insert. *SN Applied Sciences*, *2*(8), art. no. 1360. https://doi.org/10.1007/s42452-020-3167-4

[15] Barari, N., Niknam, S. A., & Mehmanparast, H. (2020). Tool wear morphology and life under various lubrication modes in turning stainless steel 316L. *Transactions of the Canadian Society for Mechanical Engineering*, *44*(3), 352-361. https://doi.org/10.1139/tcsme-2019-0051

[16] Touggui, Y., Belhadi, S., Uysal, A., Temmar, M., & Yallese, M. A. (2021). A comparative study on performance of cermet and coated carbide inserts in straight turning AISI 316L austenitic stainless steel. *International Journal of Advanced Manufacturing Technology*, *112*(1-2), 241-260. https://doi.org/10.1007/s00170-020-06385-5

[17] Dumas, M., Kermouche, G., Valiorgue, F., Van Robaeys, A., Lefebvre, F., Brosse, A., Karaouni, H., & Rech, J. (2021). Turning-induced surface integrity for a fillet radius in a 316L austenitic stainless steel. *Journal of Manufacturing Processes*, *68*, 222-230. https://doi.org/10.1016/j.jmapro.2021.05.031

[18] Del Risco-Alfonso, R., Pérez-rodríguez, R., Robledo, P. C. Z., Santana, M. R., & Quiza, R. (2021). Optimization of the cutting regime in the turning of the AISI316l steel for biomedical purposes based on the initial progression of tool wear. *Metals*, *11*(11), art. no. 1698. https://doi.org/10.3390/met11111698

[19] Benmeddour, A. (2021). Experimental investigation and numerical prediction of the effects of cutting tool geometry during turning of AISI 316l steel. *Periodica Polytechnica Mechanical Engineering*, *65*(4), 293-301. https://doi.org/10.3311/PPME.16844

[20] Martowibowo, S. Y. & Damanik, B. K. (2021). Optimization of Material Removal Rate and Surface Roughness of AISI 316L under Dry Turning Process using Genetic Algorithm. *Manufacturing Technology*, *21*(3), 373-380. https://doi.org/10.21062/mft.2021.038

[21] Leksycki, K., Feldshtein, E., & Ociepa, M. (2021). On the effect of the side flow of 316l stainless steel in the finish turning process under dry conditions. *Facta Universitatis, Series: Mechanical Engineering*, *19*(2), 335-343. https://doi.org/10.22190/FUME191118019L

[22] Szczotkarz, N., Mrugalski, R., Maruda, R. W., Królczyk, G. M., Legutko, S., Leksycki, K., Dębowski, D., & Pruncu, C. I. (2021). Cutting tool wear in turning 316L stainless steel in the conditions of minimized lubrication. *Tribology International*, *156*, art. no. 106813. https://doi.org/10.1016/j.triboint.2020.106813

[23] Benkhelifa, O., Cherfia, A., & Nouioua, M. (2022). Modeling and multi-response optimization of cutting parameters in turning of AISI 316L using RSM and desirability function approach. *International Journal of Advanced Manufacturing Technology*, *122*(3-4), 1987-2002. https://doi.org/10.1007/s00170-022-10044-2

[24] Maruda, R. W., Arkusz, K., Szczotkarz, N., Wojciechowski, S., Niesłony, P., & Królczyk, G. M. (2023). Analysis of size and concentration of nanoparticles contained in cutting fluid during turning of 316L steel in minimum quantity lubrication conditions. *Journal of Manufacturing Processes*, *87*, 106-122. https://doi.org/10.1016/j.jmapro.2022.12.065

[25] Natesh, C. P., Shashidhara, Y. M., Amarendra, H. J., Shetty, R., Harisha, S. R., Shenoy, P. V., Nayak, M., Hegde, A., Shetty, D., & Umesh, U. (2023) Tribological and Morphological Study of AISI 316L Stainless Steel during Turning under Different Lubrication Conditions. *Lubricants*, *11*(2), art. no. 52. https://doi.org/10.3390/lubricants11020052

[26] Bjerke, A., Lenrick, F., Hrechuk, A., Slipchenko, K., M'Saoubi, R., Andersson, J. M., & Bushlya, V. (2023). On chemical interactions between an inclusion engineered stainless steel (316L) and (Ti,Al)N coated tools during turning. *Wear*, *532-533*, art. no. 205093. https://doi.org/10.1016/j.wear.2023.205093

[27] Moreno, M., Andersson, J. M., M'Saoubi, R., Kryzhanivskyy, V., Johansson-Jöesaar, M. P., Johnson, L. J. S., Odén, M., & Rogström, L. (2023). Adhesive wear of TiAlN coatings during low speed turning of stainless steel 316L. *Wear*, *524-525*, art. no. 204838. https://doi.org/10.1016/j.wear.2023.204838

[28] Oussama, B., Yapan, Y. F., Uysal, A., Abdelhakim, C., & Mourad, N. (2023). Assessment of turning AISI 316L stainless steel under MWCNT-reinforced nanofluid-assisted MQL and optimization of process parameters by NSGA-II and TOPSIS. *International Journal of Advanced Manufacturing Technology*, *127*(7-8), 3855-3868. https://doi.org/10.1007/s00170-023-11747-w

Contact information:

Djordje VUKELIC, PhD
(Corresponding author)
University of Novi Sad,
Faculty of Technical Sciences,
Trg Dositeja Obradovica 6, 21000 Novi Sad, Serbia
E-mail: vukelic@uns.ac.rs

Katica SIMUNOVIC, PhD
University of Slavonski Brod,
Mechanical Engineering Faculty,
Trg Ivane Brlic Mazuranic 2, 35000 Slavonski Brod, Croatia
E-mail: ksimunovic@unisb.hr

Vitalii IVANOV, PhD
Sumy State University,
Faculty of Technical Systems and Energy Efficient Technologies,
Rymskogo-Korsakova 2, 40007 Sumy, Ukraine
E-mail: ivanov@tmvi.sumdu.edu.ua

Mario SOKAC, PhD
University of Novi Sad,
Faculty of Technical Sciences,
Trg Dositeja Obradovica 6, 21000 Novi Sad, Serbia
E-mail: marios@uns.ac.rs

Vladimir KOCOVIC, PhD
University of Kragujevac,
Faculty of Engineering,
Sestre Janjic 6, 34000 Kragujevac, Serbia
E-mail: vladimir.kocovic@kg.ac.rs

Zeljko SANTOSI, PhD
University of Novi Sad,
Faculty of Technical Sciences,
Trg Dositeja Obradovica 6, 21000 Novi Sad, Serbia
E-mail: zeljkos@uns.ac.rs

Goran SIMUNOVIC, PhD
University of Slavonski Brod,
Mechanical Engineering Faculty,
Trg Ivane Brlic Mazuranic 2, 35000 Slavonski Brod, Croatia
E-mail: gsimunovic@unisb.hr